Acta Cryst. (1956). **9**, 759

The Crystal Structure of Dickite*

BY R. E. NEWNHAM† AND G. W. BRINDLEY‡

The Pennsylvania State University, University Park, Pa., U.S.A.

(*Received* 18 *February* 1956)

The structure of dickite has been evaluated from rotation and Weissenberg data. The unit cell is monoclinic, *Cc*, $a = 5{\cdot}15$, $b = 8{\cdot}95$, $c = 14{\cdot}42$ Å, $\beta = 96°\ 48'$, and $Z = 4$. One-dimensional Fourier synthesis confirms the polar arrangement of the two kaolin layers in the unit cell. Their disposition within the cell has been established by systematic consideration of possible stacking sequences. The refined structure, obtained by two-dimensional Fourier syntheses, shows considerable distortion within the silica and alumina sheets of the structure.

1. Introduction

The determination of the structure of dickite, $Al_2Si_2O_5(OH)_4$, was undertaken as part of a program to determine the detailed crystal chemistry of the kaolin-type clay minerals. These include kaolinite, dickite, nacrite and halloysite. The basic structural scheme for these and other layer-type silicates was laid down by Pauling (1930) from crystallochemical considerations. The structures are composed of a basic unit layer, known as the kaolin layer, consisting of a hexagonal network of Si–O tetrahedra with a superposed layer of Al–O,OH octahedra. Regular sequences of one, two and six kaolin layers are found respectively in kaolinite, dickite and nacrite. Halloysite is made up of an irregular sequence of kaolin layers. From amongst these minerals, dickite alone appears to be suited to single-crystal analysis. Kaolinite and halloysite, by far the most common of the kaolin minerals, never form large crystals; at the best, kaolinite gives rise only to vermicular forms. The extremely rare nacrite, on the other hand, forms large but imperfect crystals yielding poor diffraction patterns. Dickite, however, gives sufficiently large crystals of a high degree of perfection.

An analysis of the monoclinic dickite structure was first undertaken by Gruner (1932). After obtaining the unit-cell parameters from optical data and X-ray powder photographs, he indexed the powder line diagram and noted the systematically absent reflections as *hkl* when $h+k$ is odd, *h*0*l* when *h* or *l* is odd and 0*k*0 when *k* is odd. The space group most compatible with the observed results and the nature of the kaolin layer was C_s^4–*Cc*, with the *a* and *c* axes lying in the glide plane of symmetry. The unit cell contains two kaolin layers. Gruner found two arrangements of the layers which gave identical calculated intensities for the *h*0*l* and *h*3*l* reflections, but different values for the generally weaker *h*1*l* and *h*2*l* peaks. On the basis of powder line data, however, neither structure seemed to be entirely correct.

Subsequent investigations of the structure were carried out by Ksanda & Barth (1935) and by Hendricks (1938). The former assigned dickite to the centrosymmetric space group C_{2h}^6, since the crystals appeared to be non-piezoelectric, and they also obtained single-crystal data which were compared with the theoretical values calculated from Gruner's structures, but no attempt was made to adjust the atomic coordinates to obtain better agreement. Hendricks found dickite to be pyroelectric, favoring the polar space group C_s^4. Using Ksanda & Barth's data, he refined the *z* parameters and considered various arrangements of the kaolin layers within the unit cell. He concluded that one of Gruner's original structures was most nearly correct, but many discrepancies between observed and calculated intensities still remained.

2. Experimental

Small, pseudo-hexagonal, flake-like crystals of dickite from Schuylkill, Pa., U.S.A., were used in the investigation. Rotation and Weissenberg photographs were taken about the *a* and *b* axes both of which lie in the plane of the flakes. The dimensions of the unit cell were determined from twenty reflections of the powder line diagram, using Cu $K\alpha$ radiation, $\lambda = 1{\cdot}5418$ Å. A least-squares adjustment of the unit-cell parameters yielded the following values:

$$a = 5{\cdot}15 \pm 0{\cdot}01, \quad b = 8{\cdot}95 \pm 0{\cdot}01, \quad c = 14{\cdot}42 \pm 0{\cdot}02 \text{ Å}, \quad \beta = 96°\ 48' \pm 02'.$$

The space group is C_s^4–*Cc* with $4[Al_2Si_2O_5(OH)_4]$ per unit cell. Intensities of the *h*0*l* and 0*kl* reflections were estimated visually by comparison with a calibrated scale from Weissenberg photographs, and were corrected for Lorentz and polarization factors in the usual manner. No allowance was made for absorption because of the small size of the crystals, about $0{\cdot}1 \times 0{\cdot}1 \times 0{\cdot}02$ mm.^{3}.

* Contribution No. 55–36.
† Research Fellow.
‡ Head, Department of Ceramic Technology.

3. Analysis of the structure

A preliminary one-dimensional Fourier synthesis was carried out, using nine $00l$ reflections and the z coordinates listed in Table 1. Fig. 1 compares the electron-density distribution derived from the observed intensities and calculated phase factors with the distribution obtained from the same number of calculated intensities. The close agreement between these curves confirms the mean z coordinates given in Table 1 and the polar arrangement of the two layers

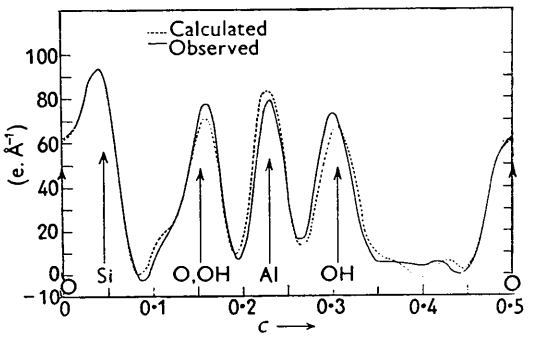

Fig. 1. One-dimensional Fourier synthesis of dickite in the c direction.

Table 1. *Mean z coordinates*

Layer	z/c
6 O	0·000
4 Si	0·042
4 O, 2 (OH)	0·153
4 Al	0·229
6 OH	0·306

in the unit cell. The calculations were made using Beevers–Lipson strips and the Bragg–West (1928) atomic scattering factors, without further allowance for thermal motion.

The analysis of the structure proceeds in two stages: (i) the determination of the stacking of the layers within the cell, and (ii) the refinement of the atomic coordinates within a layer. The first stage has been carried through using the idealized layer structure which has been amply confirmed by the earlier work. An arbitrary origin for the cell was chosen at one of the oxygen atom sites in the all-oxygen layer, at $z = 0$. There are then six possible ways of building up a single kaolin layer plus an undetermined number of additional possibilities which arise by shifting the origin in the a–b plane. The symmetry operations imposed by the space group, however, considerably reduce the number of independent structures. Suppose, for example, the origin is shifted by an amount $-X$ in the a direction and $-Y$ in the b direction. The coordinates of the ith atom in the asymmetric unit are then changed from x_i, y_i, z_i to (x_i+X), (y_i+Y), z_i. Using these new coordinates involving the arbitrary shift of origin, we proceed to investigate the form of the structure factor F, which, for a non-centrosymmetric crystal, is of the form $A+iB$. For a general hkl reflection A and B take the form

$$A(hkl) = \sum_i 4f_i \cos^2 2\pi\{\tfrac{1}{4}(h+k)\} \times \cos 2\pi(hx_i+hX+lz_i+\tfrac{1}{4}l) \cos 2\pi(ky_i+kY-\tfrac{1}{4}l) ,$$

$$B(hkl) = \sum_i 4f_i \cos^2 2\pi\{\tfrac{1}{4}(h+k)\} \times \sin 2\pi(hx_i+hX+lz_i+\tfrac{1}{4}l) \cos 2\pi(ky_i+kY-\tfrac{1}{4}l) .$$

The contributions to A and B of the original coordinates (x_i, y_i, z_i) can now be separated from those due to the superimposed movement of the origin $(-X, -Y, 0)$. For the calculated intensity, $|F_c(hkl)|^2$, we arrive at the expression

$$|F_c(hkl)|^2 = 16 \cos^4 2\pi\{\tfrac{1}{4}(h+k)\} \times \{[\cos(2\pi kY) \sum_i f_i P_i R_i - \sin(2\pi kY) \sum_i f_i P_i S_i]^2 + [\cos(2\pi kY) \sum_i f_i Q_i R_i - \sin(2\pi kY) \sum_i f_i Q_i S_i]^2\} ,$$

where (1)

$$P_i = \cos 2\pi(hx_i+lz_i+\tfrac{1}{4}l) ,$$
$$Q_i = \sin 2\pi(hx_i+lz_i+\tfrac{1}{4}l) ,$$
$$R_i = \cos 2\pi(ky_i-\tfrac{1}{4}l) ,$$
$$S_i = \sin 2\pi(ky_i-\tfrac{1}{4}l) .$$

This expression for F_c^2 is independent of X, the arbitrary shift of the origin in the a direction. Moreover, a simple calculation shows that $F_c^2(Y+\frac{1}{2}) = F_c^2(Y)$, so that only arbitrary shifts in the range $0 \leq Y < b/2$ need be considered. This limitation follows directly from the symmetry operations of the unit cell. The determination of the crystal structure is now reduced to a straightforward evaluation of (1). One need calculate only the values of P_i, Q_i, R_i, and S_i and perform the indicated summations for the six possible structures of a single kaolin layer which, when combined with the quantities $\sin 2\pi kY$ and $\cos 2\pi kY$, give the calculated intensities F_c^2. The calculated intensities can then be compared directly with the corrected observed intensities.

The six different arrangements within the kaolin layer are obtained as follows: With an oxygen atom of the all-oxygen layer at the origin, the atoms of the O layer, the Si layer and the O,(OH) layer are automatically fixed for the idealized kaolin layer. There are two ways in which the OH layer can be fitted on to the O–OH layer, which we label M and N, and three ways, a, b, and c, in which the Al atoms can be accommodated within the structure. The coordinates of the atoms making up the asymmetric unit of each of these six possibilities are listed in Table 2. The values of P_i, Q_i, R_i, and S_i were tabulated for a group of low-order reflections for each structure type.

Structures Na, Nb and Nc of Table 2 may be eliminated from further consideration by examining the $h0l$ reflections. Since the $h0l$ intensities are in-

Table 2. *Atomic coordinates of the six possible configurations of a single kaolin layer*

	Ma			*Mb*			*Mc*			*Na*			*Nb*			*Nc*		
	x/a	*y/b*	*z/c*	*x/a*	*y/b*	*z/c*	*x/a*	*y/b*	*z/c*	*x/a*	*y/b*	*z/c*	*x/a*	*y/b*	*z/c*	*x/a*	*y/b*	*z/c*
O_1	0	0	0	0	0	0	0	0	0	0	0	0	0	0	0	0	0	0
O_2	¼	¼	0	¼	¼	0	¼	¼	0	¼	¼	0	¼	¼	0	¼	¼	0
O_3	¾	¼	0	¾	¼	0	¾	¼	0	¾	¼	0	¾	¼	0	¾	¼	0
O_4	0·050	⅛	0·153	0·050	⅛	0·153	0·050	⅛	0·153	0·050	⅛	0·153	0·050	⅛	0·153	0·050	⅛	0·153
O_5	0·550	⅛	0·153	0·550	⅛	0·153	0·550	⅛	0·153	0·550	⅛	0·153	0·550	⅛	0·153	0·550	⅛	0·153
$(OH)_1$	0·550	0	0·153	0·550	0	0·153	0·550	0	0·153	0·550	0	0·153	0·550	0	0·153	0·550	0	0·153
$(OH)_2$	0·265	0	0·306	0·265	0	0·306	0·265	0	0·306	0·932	0	0·306	0·932	0	0·306	0·932	0	0·306
$(OH)_3$	0·765	⅛	0·306	0·765	⅛	0·306	0·765	⅛	0·306	0·432	⅛	0·306	0·432	⅛	0·306	0·432	⅛	0·306
$(OH)_4$	0·265	⅓	0·306	0·265	⅓	0·306	0·265	⅓	0·306	0·932	⅓	0·306	0·932	⅓	0·306	0·932	⅓	0·306
Si_1	0·014	⅛	0·042	0·014	⅛	0·042	0·014	⅛	0·042	0·014	⅛	0·042	0·014	⅛	0·042	0·014	⅛	0·042
Si_2	0·514	⅓	0·042	0·514	⅓	0·042	0·514	⅓	0·042	0·514	⅓	0·042	0·514	⅓	0·042	0·514	⅓	0·042
Al_1	0·907	0	0·229	0·907	0	0·229	0·407	⅛	0·229	0·241	0	0·229	0·241	0	0·229	0·741	⅛	0·229
Al_2	0·407	⅛	0·229	0·907	⅓	0·229	0·907	⅓	0·229	0·741	⅛	0·229	0·241	⅓	0·229	0·241	⅓	0·229

Table 3(*a*). *Comparison of 0kl structure amplitudes*

Structure		Scaled $\sqrt{F_c^2}$ values for 0*kl* reflections							*R*
Layer	*Y*(*b*/12)	020	021	022	040	060	080	0,10,0	(%)
Ma	0	31·4	20·6	52·7	24·7	104·0	6·9	9·2	23·2
Ma	1	40·4	44·0	15·5	3·0	124·6	7·2	14·7	41·8
Ma	2	2·8	40·2	46·4	29·9	113·0	14·1	3·3	37·1
Mc	0	70·3	0·0	27·0	5·5	108·4	12·8	25·5	53·5
Mc	1	39·3	48·7	15·1	3·0	121·0	7·0	14·3	42·3
	F_o	21·6	35·3	59·3	9·6	100·0	7·4	16·3	—

Table 3(*b*). *Comparison of 11l structure amplitudes*

Structure		Scaled $\sqrt{F_c^2}$ values for 11*l* reflections							*R*
Layer	*Y*(*b*/12)	110	11$\bar{1}$	111	11$\bar{2}$	112	11$\bar{3}$	113	(%)
Ma	0	8·6	4·8	4·7	3·5	9·4	4·5	4·4	43·6
Mb	0								
Ma	3	4·6	4·4	10·5	4·5	4·4	5·3	6·2	23·0
Mb	3								
	F_o	6·1	6·8	8·8	4·8	3·9	5·7	3·8	—

dependent of Y, their values for the six structure types fall into two groups corresponding to the M and N structures. Calculations were carried out for 39 $h0l$ reflections. The M-type structures gave an agreement factor ($R = |F_o - F_c|/|F_c|$) of 24·5% while the N-type structures gave $R = 45{\cdot}4\%$, indicating considerably less agreement with experiment and thus eliminating them from further consideration.

We consider next the various values of Y between 0 and $b/2$. Although in theory Y can take any value within this range, it is possible to limit the number of trial values through consideration of the strong 060 reflection. With an arbitrary division of the cell into increments of $b/24$, it is obvious that the calculated intensity of 060 is zero whenever Y is an odd multiple of $b/24$; thus, to a first approximation, it may be assumed that Y is an even multiple of $b/24$. The values of F_c^2 for the three M-type structures were computed for certain low-order 0kl reflections using the following values for Y: 0, $b/12$, $b/6$, $b/4$, $b/3$, and $5b/12$. These eighteen possible structures yield only five different sets of 0kl intensities. The results of calculation are given in Table 3(*a*), where the calculated intensities are scaled to the corresponding observed quantities. The structure type *Ma*, $Y = 0$, gives an R-factor appreciably lower than any of the other four possibilities, thus eliminating them. There are, however, three other structures (*Ma*−3, *Mb*−0 and *Mb*−3) giving the same set of 0kl intensities as *Ma*−0. These were differentiated on the basis of a group of 11l intensities (see Table 3(*b*)). Finally, then, two structures remain, *Ma*−3 and *Mb*−3, giving identical calculated intensities for all reflections. These structures can be superposed by a shift of $x = a/2$ and $z = c/2$, which in no way affects the calculated intensities. Hence the two structures may be considered identical. The refinement of the *Ma*−3 structure is discussed in the following section.

4. Refinement of the atomic parameters

The refinement of the *Ma*−3 structure was carried out on X-RAC using two-dimensional projections of the *a*–*c* and *b*–*c* planes. The Fourier summation of the electron-density projection along [100] was taken over 86 non-zero 0kl reflections. Eleven of the thirteen

Table 4. *Atomic coordinates for the preliminary and refined structures*

Atom	A. Preliminary coordinates			B. Refined coordinates		
	x/a	*y/b*	*z/c*	*x/a*	*y/b*	*z/c*
O_1	0·000	0·250	0·000	−0·039	0·242	−0·009
O_2	0·250	0·500	0·000	0·263	0·459	0·001
O_3	0·750	0·500	0·000	0·773	0·509	0·001
O_4	0·050	0·417	0·153	0·088	0·383	0·152
O_5	0·550	0·583	0·153	0·528	0·582	0·157
$(OH)_1$	0·550	0·250	0·153	0·588	0·276	0·157
$(OH)_2$	0·265	0·250	0·306	0·270	0·264	0·302
$(OH)_3$	0·765	0·417	0·306	0·770	0·407	0·299
$(OH)_4$	0·265	0·583	0·306	0·305	0·584	0·300
Si_1	0·014	0·417	0·042	0·005	0·402	0·041
Si_2	0·514	0·583	0·042	0·505	0·580	0·040
Al_1	0·907	0·250	0·229	0·918	0·250	0·233
Al_2	0·407	0·417	0·229	0·418	0·419	0·232

Table 5. *Observed and calculated structure factors*

0*kl*	F_o	F_c	0*kl*	F_o	F_c	0*kl*	F_o	F_c	0*kl*	F_o	F_c
002	20·7	26·6	044	17·0	15·5	081	12·4	7·2	2,0,16	15·7	21·1
004	37·5	43·6	045	13·3	11·1	082	1·4	2·4	20$\bar{2}$	30·7	24·8
006	24·1	24·1	046	3·6	6·5	083	3·1	4·2	20$\bar{4}$	18·3	18·3
008	23·6	21·3	047	14·5	12·0	084	4·4	4·1	20$\bar{6}$	20·6	19·4
0,0,10	20·3	18·7	048	21·2	19·4	085	4·4	3·0	20$\bar{8}$	23·9	23·0
0,0,12	22·6	21·4	049	11·8	11·1	086	3·1	3·2	2,0,$\bar{10}$	38·0	43·1
0,0,14	14·4	14·5	0,4,10	11·4	11·5	087	2·2	2·7	2,0,$\bar{12}$	8·2	5·5
0,0,16	22·0	21·7	0,4,11	1·4	1·1	088	4·1	6·7	2,0,$\bar{14}$	16·5	19·2
0,0,18	4·9	3·8	0,4,12	13·2	12·8	089	2·8	1·7	2,0,$\bar{16}$	4·6	7·3
			0,4,13	2·2	4·3	0,8,10	1·7	1·7	2,0,$\bar{18}$	10·4	8·3
020	9·2	8·0	0,4,14	3·9	7·9	0,8,11	8·6	5·6			
021	14·9	14·7	0,4,15	0·0	0·0	0,8,12	5·4	4·6	400	25·5	17·6
022	25·0	20·8	0,4,16	3·0	6·1	0,8,13	0·0	2·4	402	25·3	19·5
023	8·6	6·9	0,4,17	2·2	4·4				404	6·0	7·3
024	13·0	13·8				0,10,0	6·9	4·8	406	24·0	26·1
025	6·0	6·5	060	42·3	42·6	0,10,1	7·4	4·7	408	19·2	21·3
026	10·2	10·4	061	6·6	4·1	0,10,2	2·6	6·6	4,0,10	5·1	7·9
027	2·2	3·3	062	18·0	14·5	0,10,3	5·7	6·6	4,0,12	11·3	13·4
028	9·8	9·7	063	7·9	4·5	0,10,4	6·0	6·7	40$\bar{2}$	29·0	21·5
029	4·6	6·2	064	17·4	19·4	0,10,5	2·5	3·6	40$\bar{4}$	39·2	32·1
0,2,10	1·9	2·4	065	5·0	3·1	0,10,6	2·2	4·2	40$\bar{6}$	8·4	6·1
0,2,11	6·7	6·2	066	14·6	11·5	0,10,7	10·1	9·8	40$\bar{8}$	28·2	26·7
0,2,12	6·2	7·3	067	6·1	3·9	0,10,8	9·2	9·8	4,0,$\bar{10}$	8·4	8·1
0,2,13	6·3	5·8	068	8·8	9·1	0,10,9	6·9	7·0	4,0,$\bar{12}$	5·2	8·6
0,2,14	6·1	4·0	069	4·4	5·1				4,0,$\bar{14}$	7·8	10·8
0,2,15	4·0	3·7	0,6,10	18·0	17·6	200	27·3	22·2			
0,2,16	0·0	0·8	0,6,11	3·0	4·7	202	42·2	39·6	600	5·2	4·6
0,2,17	2·8	3·7	0,6,12	16·4	14·5	204	31·4	32·8	602	12·8	11·7
0,2,18	3·4	3·8	0,6,13	2·8	4·3	206	38·0	38·6	604	7·9	6·3
			0,6,14	10·8	10·9	208	15·5	13·2	60$\bar{2}$	19·0	19·3
040	4·1	2·1	0,6,15	1·7	2·3	2,0,10	18·6	17·8	60$\bar{4}$	15·0	14·1
041	2·8	1·0				2,0,12	13·3	15·0	60$\bar{6}$	10·5	5·7
042	7·2	7·0	080	3·1	4·3	2,0,14	5·3	5·0	60$\bar{8}$	15·7	14·2
043	7·4	9·3									

atoms in the asymmetric unit were clearly resolved, and the projection was refined by the 'back-shift' method, using the observed and calculated electron-density maps. The initial y and z coordinates and the final values, after three successive Fourier refinements, are listed in Table 4. The y coordinates of atoms O_2 and O_3, which are not resolved in projection, were obtained by minimizing the R factor for various separations. The electron-density map for the third 0*kl* refinement is shown in Fig. 2(*a*).

The overlap of the atomic peaks in the (010) projection makes refinement of the x coordinates by two-dimensional Fourier methods extremely difficult. Three refinements of the *h*0*l* projection (Fig. 2(*b*)) yielded a set of average x parameters for overlapping atoms. The agreement between the observed and calculated intensities was improved still further by splitting the x coordinates of overlapping atoms while still retaining the same average values. The initial and final x parameters are listed in Table 4.

Table 5 compares the observed structure amplitudes with the corresponding theoretical values calculated from the atomic coordinates given in Table 4. The 86 0*kl* reflections yield an R factor of 16·6% while the 39 *h*0*l* reflections give R = 14·8%.

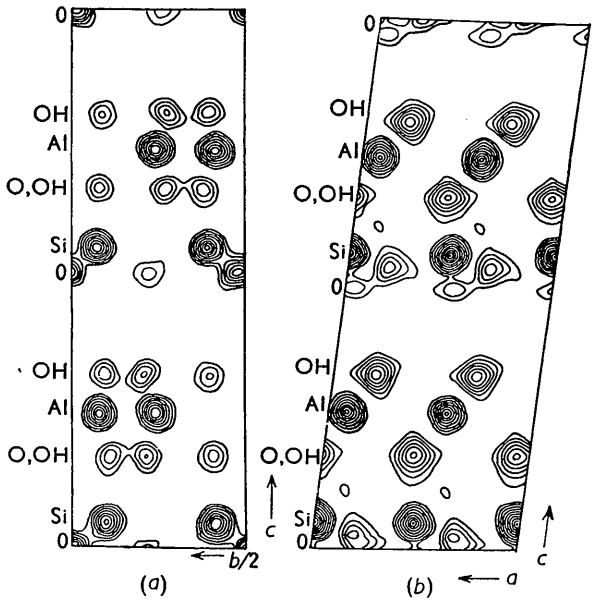

Fig. 2. Fourier syntheses of the dickite structure projected (*a*) parallel to the *a* axis, (*b*) parallel to the *b* axis.

5. Discussion of the structure

The Si–O and Al–O,(OH) distances are summarized in Table 6. The average bond lengths, Si–O = 1·64 Å and Al–O,(OH) = 1·94 Å, may be compared with the corresponding values, namely 1·59 and 2·03 Å, calculated for the idealized layer structure. The distortion of the actual layer from the idealized arrangement reduces the Al bonds to values in better agreement with those usually found, and the increase in the Si bond lengths is also acceptable. As Pauling (1930) and others have pointed out, there is a considerable misfit between the octahedral aluminum layer as found in gibbsite, where the parameter corresponding to *b* is 8·64 Å, and an ideal hexagonal net of tetrahedra with Si–O = 1·62 Å, which has a value of *b* = 9·16 Å. We see that in dickite the 'oversized' silica layer is compressed mainly by rotations of the tetrahedra (see Fig. 3(*a*)), while the alumina layer, though expanded, is not expanded by so large amount as the idealized arrangement required, and the principal distortion is a shortening of the shared octahedral edges in accordance with Pauling's rules (see Fig. 3(*b*)).

Table 6. *Interatomic distances*

Si_1–O_1	1·60 Å	Si_2–O_1	1·61 Å
Si_1–O_2	1·62	Si_2–O_2	1·63
Si_1–O_3	1·64	Si_2–O_3	1·66
Si_1–O_4	1·67	Si_2–O_5	1·67
Average Si–O, 1·638 Å.			
Al_1–O_4	1·94 Å	Al_2–O_4	1·96 Å
Al_1–O_5	1·98	Al_2–O_5	1·94
Al_1–$(OH)_1$	1·93	Al_2–$(OH)_1$	1·94
Al_1–$(OH)_2$	1·97	Al_2–$(OH)_2$	1·92
Al_1–$(OH)_3$	1·90	Al_2–$(OH)_3$	1·95
Al_1–$(OH)_4$	1·90	Al_2–$(OH)_4$	1·91
Average Al–O,(OH), 1·937 Å.			

The interlayer bonding is illustrated in Fig. 4, which shows the oxygen–hydroxyl stacking found between successive kaolin layers in the refined dickite structure. Each oxygen atom is paired off with one

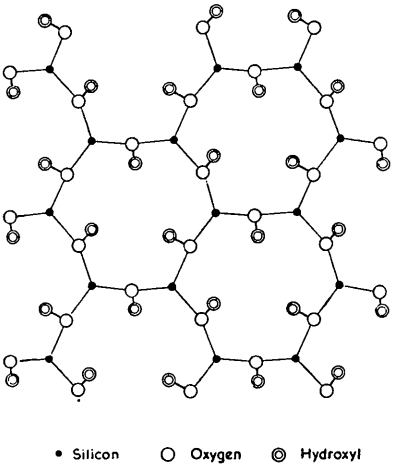

Fig. 4. Projection on (001) of adjacent Si–O network and OH layer, showing pairing of oxygens and hydroxyls.

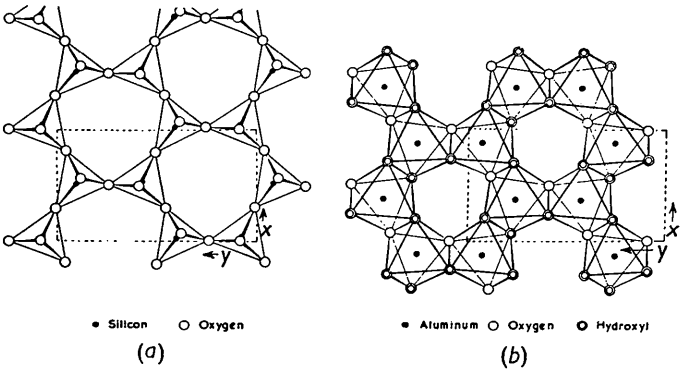

Fig. 3. Projections on (001) of (*a*) the Si–O tetrahedral layer and (*b*) the Al–O(OH) octahedral layer.

hydroxyl in the adjacent layer. The average O–OH interatomic distance is 2·89 Å, indicating the presence of hydroxyl-type bonding between the kaolin layers.

Finally we desire to thank Prof. Ray Pepinsky for making available the facilities of X-RAC, and Prof. V. Vand, Dr P. F. Eiland, Mrs Josephine Lombard and Mr H. A. McKinstry for numerous discussions. We also wish to record our indebtedness to the Gulf Research and Development Company for the financial support which made this investigation possible.

References

BRAGG, W. L. & WEST, J. (1928). *Z. Kristallogr.* **69**, 118.
GRUNER, J. W. (1932). *Z. Kristallogr.* **83**, 394.
HENDRICKS, S. B. (1938). *Amer. Min.* **23**, 863.
KSANDA, C. J. & BARTH, T. F. W. (1935). *Amer. Min.* **20**, 631.
PAULING, L. (1930). *Proc. Nat. Acad. Sci., Wash.* **16**, 123.

Acta Cryst. (1956). **9**, 764

Packing in Framework Structures*

BY WILLIAM T. HOLSER

Institute of Geophysics, University of California, Los Angeles 24, *California, U.S.A.*

(*Received* 27 *February* 1956)

The topology of framework structures as described recently by Wells is considered in relation to packing coefficient. For stacked nets of regular polygons the packing decreases with the rank and proportion of the large polygon. In framework silicates, however, large polygons such as the 8-gons in feldspar are stable only in a collapsed form with diameter similar to 6-gons, and the resulting increase in packing may more than offset the topological effect. Four-connected silicate frameworks with packings appreciably greater than that of quartz are not likely.

Introduction

A general survey of possible structural arrangements in crystals was first given by Niggli (summarized in Niggli, 1941), who enumerated them on the basis of the type and arrangement of coordination polyhedra and the number of dimensions in the structural complex.

More recently Wells (1954*a*, *b*, *c*, *d*, 1955) has discussed the possible extended networks from a more strictly topological viewpoint, with particular emphasis on the proportions of polygons of various numbers of sides (here called *rank*) formed by connecting points at the centers of atoms. Wells (1954*d*) also noted the variation in packing of a framework structure with the coordination number; in terms of packing coefficient (percentage of space filled by spherical atoms; 10 times the 'packing index' of Fairbairn (1943)) representative values are:

Coordination number	Packing coefficient (%)
12	74
8	68
6	52
4	34
3	23

* Publication No. 67, Institute of Geophysics, University of California, Los Angeles 24, California, U.S.A.

† The term *net* as used by Wells is not restricted to its standard crystallographic usage (International Union of Crystallography, 1952) as Wells' points are not necessarily symmetrically equivalent.

These considerations raise a question as to the relative importance of other variables in the packing, and in particular the possible relation of packing to the polygonal topology of the structure. In the following discussion the theoretical relations are compared with actual packings found in some known silicate framework structures. Elsewhere (Holser & Schneer, 1956) these conclusions are applied as part of a discussion of possible polymorphic transformations under the high pressures in the earth's mantle.

Packing in two-dimensional nets

We restrict the present discussion to three-dimensional 4-connected nets.† As pointed out by Wells (1954*b*, *c*), silicate or other tetrahedral frameworks that have coordination numbers 4,2 form frameworks that are topologically equivalent to these nets. One of the ways (Wells, 1954*b*) in which three-dimensional 4-connected nets may be formed is by stacking two-dimensional 3-connected nets and connecting them with additional links to each point. Wells has derived systematically 15 of these latter nets, as enumerated in Table 1 and Fig. 1 of his paper (1954*a*). Consider now the packing coefficient (in two dimensions) of these nets. Of course it will vary with the lengths and angles of the bonds, neither of which is of topological consequence. Even with the restriction of periodicity, a wide variation is possible. As a preliminary step let us form the nets from polygons which are as regular (symmetrical, with bonds of equal length) as possible, although in certain